

VIP Very Important Paper



Discovery of Antimicrobial Lipodepsipeptides Produced by a *Serratia* sp. within Mosquito Microbiomes

Jack G. Ganley^{+, [a]}, Gavin Carr^{+, [b]}, Thomas R. Ioerger,^[c] James C. Sacchettini,^[d] Jon Clardy,^{*, [b]} and Emily R. Derbyshire^{*, [a]}

The *Anopheles* mosquito that harbors the *Plasmodium* parasite contains a microbiota that can influence both the vector and the parasite. In recent years, insect-associated microbes have highlighted the untapped potential of exploiting interspecies interactions to discover bioactive compounds. In this study, we report the discovery of nonribosomal lipodepsipeptides that are produced by a *Serratia* sp. within the midgut and salivary glands of *Anopheles stephensi* mosquitoes. The lipodepsipeptides, stephensiolides A–K, have antibiotic activity and facilitate bacterial surface motility. Bioinformatic analyses indicate that the stephensiolides are ubiquitous in nature and are likely important for *Serratia* spp. colonization within mosquitoes, humans, and other ecological niches. Our results demonstrate the usefulness of probing insect–microbiome interactions, enhance our understanding of the chemical ecology within *Anopheles* mosquitoes, and provide a secondary-metabolite scaffold for further investigation of this complex relationship.

Insects accommodate diverse bacterial symbionts with the ability to produce complex secondary metabolites. Elucidation of these natural products has advanced our understanding of complex interspecies relationships.^[1–4] Of the thousands of known insect families, we are particularly interested in mosquitoes that transmit infectious agents. The diseases associated with these agents include malaria, Zika fever, dengue fever and chikungunya.^[5] Our specific interests are with *Anopheles* mosquitoes, the main vectors for the transmission of the *Plasmodium* parasite, the causal agent of malaria. Previous studies have revealed that the *Anopheles* microbiome influences the vector and the *Plasmodium* parasite by mechanisms that are

not fully understood.^[6] Recently, some of the molecular processes behind this symbiotic relationship have been unveiled.^[7] For instance, microbiome members can indirectly reduce the *Plasmodium* parasite load by stimulating the mosquito's immune response,^[8] or directly modulate the parasite by producing reactive oxygen species.^[9] However, natural products synthesized by microbes within *Anopheles* mosquitoes have remained widely unexplored. In this report, we characterize 11 new microbiome-associated lipodepsipeptide antibiotics, stephensiolides A–K (1–11), that are produced within *Anopheles* mosquitoes. Our findings provide a mosquito-microbiome natural product scaffold to allow further study of the chemical ecology within this deadly insect.

As *Plasmodium* parasites are introduced into both the midgut and the salivary glands during their life cycle, we aimed to isolate bacterial species from both tissues. First, the salivary glands and midguts were dissected from 50 female and 50 male *A. stephensi* mosquitoes, and plated individually on lysogeny broth (LB) agar plates. Analysis of the isolates by 16S rRNA gene sequencing revealed that two predominant bacterial strains had been isolated. One strain, a Gram-negative bacterium 99% identical in sequence to *Serratia marcescens* Db11 was found in both female and male mosquitoes.^[10] Though this isolate had previously been identified in mosquito midguts,^[11] here it was additionally found to be abundant in *Anopheles* salivary glands. The other isolate identified was similar to *Elizabethkingia anophelis*, a common mosquito-microbiome strain, that is associated with *Anopheles* midguts and salivary glands.^[12,13] Because *Serratia* spp. are well established as natural product producers,^[14] we further investigated the biosynthetic potential of this isolated strain.

Mass spectrometry analysis of monoculture *Serratia* sp. extracts uncovered a variety of masses ranging from 599 to 695 Da. The compounds were isolated, and the structure of stephensiolide F (**6**) was determined. This metabolite had a molecular ion peak at m/z 668.4343 in the HRMS (ESI+) spectrum, which is consistent with a molecular formula of $C_{33}H_{57}N_5O_9$. Analysis of the 1D and 2D NMR spectra for **6** indicated the presence of five amino acids: threonine, valine, isoleucine and two serine residues. A large aliphatic peak in the ¹H NMR spectrum suggested the presence of a long alkyl chain typical of lipopeptides. HMBC correlations indicated that the nitrogen atom of the threonine was acylated with this alkyl chain; the shift of Thr-H β suggested that the hydroxy group of threonine was esterified. Further HMBC correlations support the threonine being linked to an isoleucine via an ester bond and to a serine through an amide bond. The positions of the

[a] J. G. Ganley,⁺ Prof. E. R. Derbyshire
Department of Chemistry, Duke University
124 Science Drive, Durham, NC 27708-0346 (USA)
E-mail: emily.derbyshire@duke.edu

[b] Dr. G. Carr,⁺ Prof. J. Clardy
Department of Biological Chemistry and Molecular Pharmacology
Harvard Medical School
240 Longwood Avenue, Boston, MA 02115 (USA)
E-mail: jon_clardy@hms.harvard.edu

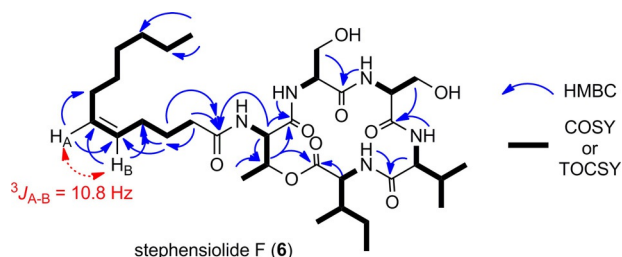
[c] Prof. T. R. Ioerger
Department of Computer Science, Texas A&M University
College Station, TX, 77843 (USA)

[d] Prof. J. C. Sacchettini
Department of Biochemistry and Biophysics, Texas A&M University
College Station, TX 77843 (USA)

[*] These authors contributed equally to this work.

Supporting information and the ORCID identification numbers for the authors of this article can be found under <https://doi.org/10.1002/cbic.201800124>.

remaining serine and valine residues were determined by NH-H α gCOSY correlations and NH/H α /H β HMBC correlations to the respective carbonyl groups. The major NMR correlations are outlined in Scheme 1. Olefinic signals in the ^1H NMR spectrum for **6** suggested the presence of a double bond within the lipid side chain. The location of this double bond was determined by HMBC correlations to be between the fifth and sixth carbons in the chain. The ^{13}C shifts of the vinyl carbons^[15] along with the coupling constants between the sp^2 protons^[16] (10.8 Hz) suggest the *Z* isomer (Table S1 in the Supporting Information).



Scheme 1. Major NMR correlations for determining the structure of stephensiolide F (**6**) along with the observed $^3J_{\text{A-B}}$ coupling constant between the olefinic protons.

Stephensiolide I (**9**) gave a peak in the HRMS (ESI+) spectrum at m/z 670.4387, which is consistent with a molecular formula of $\text{C}_{33}\text{H}_{59}\text{N}_5\text{O}_9$; this differs from the molecular formula of **6** by the addition of two hydrogen atoms. The 1D and 2D NMR spectra of **9** were similar to those of **6**, with the major difference being the absence of the olefinic signals (Table S2). The gCOSY and HMBC correlations and MS/MS suggested the same peptide sequence, but the configuration of these amino acids was still unknown. Partial hydrolysis of **9** followed by Marfey's analysis^[17] indicated the presence of L-serine, D-serine, D-valine, L-isoleucine and L-threonine. However, assignment of these residues remained ambiguous due to the presence of both L- and D-serine. Therefore, a small sample of **9** was partially hydrolyzed, and a fragment with mass 317 Da was purified by HPLC (Scheme S1). Marfey's analysis of this fragment revealed the presence of L-isoleucine, D-valine and L-serine, thus indicating that L-serine is linked to D-valine and therefore D-serine must be linked to L-threonine. Thus, by utilizing a combination of methods, we were able to completely assign the structure of **9**. As **6** contained the same amino acid sequence as **9**, based on biosynthetic considerations, it was expected to have the same absolute configuration of amino acids as **9**.

HRMS (ESI+) and MS/MS analysis of stephensiolides A (**1**), C (**3**), E (**5**), and G (**7**) revealed that these structures contained a valine instead of a isoleucine at the fifth amino acid position. This was further confirmed by analysis of the 1D and 2D NMR data. Marfey's analysis of **7** indicated the presence of both L- and D-valine, along with L-threonine and L- and D-serine. Biosynthetic considerations indicated that **1**, **3**, **5**, and **7** should have the same absolute configuration of amino acids as **9**, thus suggesting that D-valine is linked to L-serine, whereas L-valine is linked to L-threonine. The structures of the remaining

stephensiolides could be determined from their molecular formula and by comparing their NMR and/or MS/MS data with the data for the compounds above (see the Supporting Information for all NMR and MS/MS spectra). The diversity in the structures of the stephensiolides results from the length of the acyl chain, the presence or absence of a double bond in the acyl chain, and the presence of either isoleucine or valine at the fourth and fifth amino acid positions (Figure 1 A). The absolute configuration of the amino acids in the remaining stephensiolides was expected to be the same as in **9**.

To determine the biosynthetic origin of the stephensiolides, the genome of the *Anopheles*-associated *Serratia* sp. was sequenced. The stephensiolides contain both D- and L- amino acids and are cyclized through a macrolactone ring, both of which are hallmarks of nonribosomal peptide synthetases (NRPS).^[18] Based on our bioinformatic analysis, only one candidate NRPS that could produce the stephensiolides was identi-

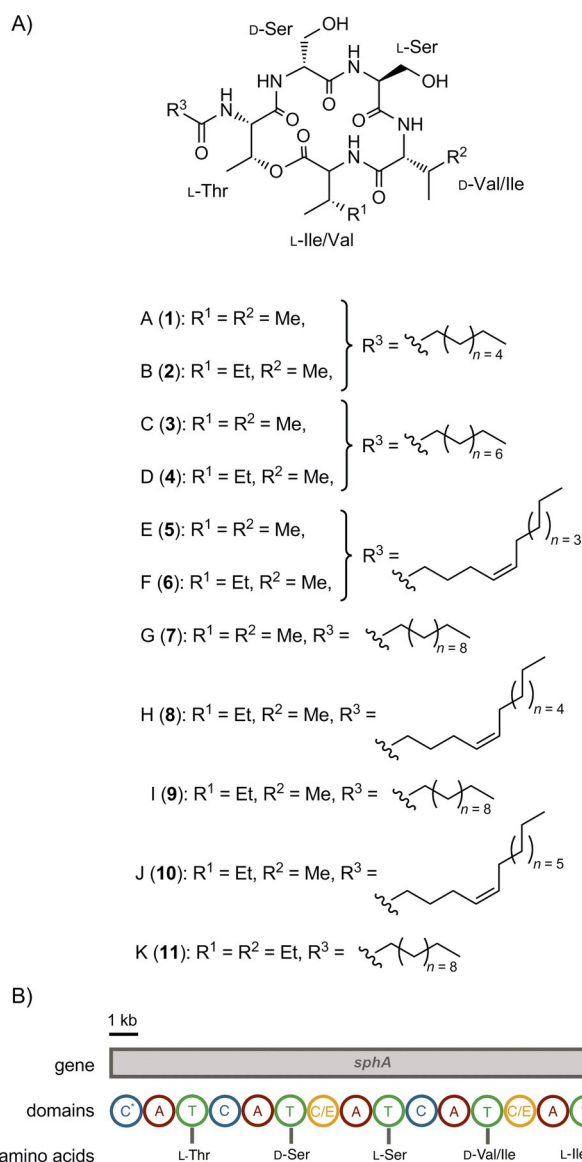


Figure 1. A) Structures of the 11 stephensiolides. B) The single 17.85 kb NRPS gene, the catalytic domains encoded, and the corresponding amino acids.

fied; it was named SphA (5950 amino acids). This NRPS consists of five modules each containing condensation (C), adenylation (A), and thiolation (T) domains, and one terminal thioesterase (TE) domain (Figure 1B). Based on the prediction informatics for secondary metabolites (PRISM) algorithm,^[19] SphA contains an initial C domain that is homologous to the fatty-acid-loading C domain of EndA, which catalyzes the initial N-acylation of D-Asp in the biosynthesis of enduracidin.^[20] EndA and SphA likely use a corresponding CoA-activated fatty acid as the starter unit; this accounts for the N-acylated carbon chains in the enduracidin and stephensiolid structures. The substrate specificity prediction of the five adenylation domains are Thr, Ser, Ser, Val and Val; this is in accordance with four of the eleven stephensiolid structures. As both the fourth and fifth positions contain either valine or isoleucine, it is likely that there is low specificity between these two amino acids, thus indicating promiscuity in the fourth and fifth A domains. The PRISM and antiSMASH^[21] algorithms additionally predicted the third and fifth C domains to be dual condensation/epimerization (C/E) domains, as recognized by the presence of the consensus sequence motif HHI/LxxxxGD (Figure S1).^[22,23] This bioinformatic analysis supports SphA's being the NRPS responsible for the biosynthesis of the stephensiolides (Figure S2).

With the structures of the stephensiolides characterized and their biosynthetic origin resolved, we next probed the biological relevance of these metabolites by exploring their production in mosquitoes. *A. stephensi* mosquitoes were washed briefly with water and ethanol to remove possible surface microbes or contaminants, ground with a mortar and pestle, and extracted with methanol, then the extract was analyzed by HRMS (ESI+). All 11 stephensiolid masses were extracted from the *A. stephensi* sample by using mass ion extraction, and compared to *Serratia* sp. extracts (Figure 2). A calibration curve was then generated for stephensiolid F (**6**), the most abundant stephensiolid within mosquitoes. Upon evaluation of two separate samples of mosquitoes (≈ 100 – 200 mosquitoes/sample), we estimated the average stephensiolid F (**6**) concentration to be 1.9 ng/mosquito or $1.2 \mu\text{g mL}^{-1}$ (Figure S3). After the mosquito extracts had been compared to the *Serratia* sp. culture, it appeared that the relative production of each stephensiolid varies. As in the mosquito extracts, all 11 of the stephensiolides were detected with identical retention times (Figure S4), therefore the entire repertoire of stephensiolides is

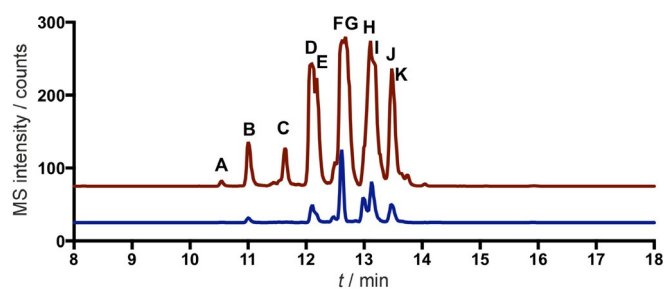


Figure 2. Extracted ion chromatogram of the masses of all 11 stephensiolid of extracts from both *A. stephensi* mosquitoes (—) and *Serratia* sp. culture (—).

synthesized within the mosquito host. The relative differences in stephensiolid abundances in nutrient broth versus in the mosquito might be due to the different substrate pools or differences in enzyme activity under native versus artificial growth conditions. Additionally, *Anopheles* midguts are likely alkaline,^[24] whereas our artificial growth conditions are neutral; this could also account for these differences.

We were interested in potential bioactivities for stephensiolides because they are produced within mosquitoes. Within laboratory and field-caught *A. stephensi* mosquitoes, Gram-negative γ -proteobacteria such as *Serratia* are the most abundant class of bacteria.^[11] Although there are only a few examples to date, some Gram-negative bacteria have been shown to be symbionts of mosquitoes.^[25,26] To assess the ability of the stephensiolides to modulate Gram-negative bacteria, in vitro activity assays were conducted (Table 1). First, the stephensiolid mixture was tested against the *A. stephensi*-associated Gram-negative bacterium *Elizabethkingia* sp., one of the most common bacteria within *A. stephensi*.^[11] The stephensiolid mixture did not inhibit this strain or the common Gram-negative laboratory strain *Escherichia coli* K12 up to $200 \mu\text{g mL}^{-1}$.

Table 1. Activity of the stephensiolides.

Cell type	Cell line	IC ₅₀ [$\mu\text{g mL}^{-1}$]
Gram-positive bacteria	<i>B. subtilis</i> 3610	15
Gram-negative bacteria	<i>E. coli</i> K12	200
human hepatocytes	HepG2	21
protozoan parasites	<i>P. falciparum</i> Dd2	14
mosquito commensal	<i>Elizabethkingia</i> sp.	> 200

The mixture was also tested against the common Gram-positive laboratory strain *Bacillus subtilis* 3610, which was inhibited with an IC₅₀ of $15 \mu\text{g mL}^{-1}$. We further determined the minimum inhibitory concentration (MIC)^[27] of **6** against *B. subtilis* ($> 32 \mu\text{g mL}^{-1}$) and found it to be less potent than the FDA-approved lipodepsipeptide, daptomycin (MIC = 0.5 – $1.0 \mu\text{g mL}^{-1}$).^[28] However, our calculated concentration of **6** within mosquitoes is approximately ten times less than the IC₅₀, thus suggesting that this inhibition could be physiologically relevant. Intriguingly, multiple Gram-positive bacteria, including *B. subtilis*, *Bacillus thuringiensis*, *Lysinibacillus sphaericus* and *Clostridium bif fermentens*, have been shown to be entomopathogenic.^[29–32] This suggests that the stephensiolides might aid *A. stephensi* mosquitoes in combating entomopathogenic bacteria, as well as rationalize the overwhelming presence of Gram-negative bacteria over Gram-positive bacteria within *A. stephensi*. However, examination of this functional role in mosquitoes awaits tests with live insects. The activity of stephensiolides against malaria parasites was also evaluated. The stephensiolid mixture inhibited *Plasmodium falciparum* Dd2 blood-stage parasites with an IC₅₀ value of $14 \mu\text{g mL}^{-1}$ (Table 1), similar to its observed inhibition of human hepatocytes (IC₅₀ = $21 \mu\text{g mL}^{-1}$).

A bioinformatic analysis of similar natural-product gene clusters was performed. Comparison of the *sphA* cluster to known

Serratia natural-product genes or gene clusters revealed that the genes encoding for serrawettin W2 (*swrA*) and serrawettin W1/serratomolide (*swrW*) peptide synthetases have high sequence homology to *sphA* (78% identity, 82–83% coverage and 70% identity, 34% coverage, respectively).^[33,34] The serrawettin W2 NRPS has a similar domain architecture to that of the stephensiolide cluster, with five modules each containing C, A and T domains, followed by a terminal TE domain. Furthermore, two of the five A domains of SwrA match substrate specificity to SphA. The overall structure of serrawettin W2 mimics the stephensiolide core structure, including a cyclic pentapeptide structure with adjacent hydrophobic amino acids flanking polar amino acids. Specifically, the peptide sequence of serrawettin W2 is Leu-Ser-Thr-Phe-Ile; the stephensiolide peptide sequence is Thr-Ser-Ser-Val/Ile-Ile/Val. An additional difference is that the serrawettin W2 lactone is cyclized through a 3-hydroxy group of the fatty acid, whereas the stephensiolides are cyclized through the hydroxy group of the threonine (Figure S5).

Given the hydrophobic tails and hydrophilic head groups of the serrawettins, they unsurprisingly function as biosurfactants,^[33,35] which aid in bacterial swarming motility. Swarming motility facilitates the translocation of bacterial populations across a solid surface and is often critical for pathogenicity and infection.^[36] Due to the sequence homology between the NRPS clusters and the structural similarities between the stephensiolides and the serrawettins, we hypothesized that the stephensiolides function as biosurfactants. We first tested the ability of *Serratia* sp. to swarm on semi-solid media and observed swarming at 30 °C (Figure 3A). To ascertain that the swarming movement was not a result of serrawettin production, the *Serratia* sp. genome was searched; no clear homologue for *swrA* or *swrW* was present. Furthermore, EtOAc ex-

tracts of the *Serratia* sp. were analyzed, and neither serrawettin molecular ion was present (Figure S6). The biosurfactant potential of stephensiolides was tested by adding the mixture to the wild-type (WT) strain and then measuring swarming motility hourly for 13 hours post-inoculation. A significant increase in swarming compared to the DMSO vehicle control was observed from 9–13 hours post-inoculation (Figure 3B).

The effect of the stephensiolide mixture on *Serratia* sp. growth was also assessed to determine if this could influence swarming. Stephensiolides do not affect bacterial growth, thus indicating that the swarming phenotype was not a result of accelerated growth upon treatment (Figure S7). To confirm the stephensiolides' role in swarming motility, a non-swarming *S. marcescens* strain (CMS635, *swrW*::Tn)^[37] that is incapable of producing serrawettin W1 was inoculated on swarming plates with and without the stephensiolide mixture. Addition of the stephensiolides restored swarming levels of the *swrW* mutant to a level comparable to that of the WT strain *S. marcescens* CMS376 (Figure 3C–E). Together these results support the proposal that stephensiolides facilitate swarming motility as biosurfactants. The overall significance of swarming motility within mosquitoes is not completely understood; however, it is possible that an enhanced swarming ability allows for colonization and migration of multiple different tissues within the insect host. Recently, a very similar *Serratia* sp. has been shown to infect multiple different tissues within mosquitoes, including reproductive organs.^[38]

The geographic and ecological distribution of organisms with the stephensiolide gene cluster (*sphA*) was evaluated. Basic local alignment search tool (BLAST) analysis^[39] of the entire *sphA* gene identified seven other sequenced *Serratia* spp. containing a homologue with an identical predicted domain architecture to SphA (Figures S8). These strains were mapped and distinguished by their isolation source (Figure S9). Four of the seven *Serratia* spp. were from hospital patients in the United States, Mexico, Germany, and Japan. Over the past few decades, *Serratia* spp. have emerged as important opportunistic pathogens, often the result of intensive care unit infections, and are among the top pneumonia-causing bacteria.^[40] As biosurfactants often aid in colonization and infection,^[36] the stephensiolides might be relevant to understanding *Serratia* pathogenesis in humans. Two additional strains isolated from nematode and plant endosymbionts were shown to have the *sphA* gene, further showing that the stephensiolides do not appear to be restricted to a specific niche. Interestingly, the *sphA* gene is also present in the previously mentioned *Serratia* sp. that infects the reproductive tissues within *A. stephensi* mosquitoes.^[38] Because environmentally acquired microbiome members in *A. stephensi* have been shown to be moderately dynamic,^[11] the discovery of the stephensiolide cluster in additional mosquito samples suggests that stephensiolides could be present across broad mosquito populations. Additionally, the presence of the cluster from strains with various hosts suggests an important conserved function for the compounds.

In conclusion, we have reported the structure and characterization of the stephensiolides, a new natural product scaffold isolated from bacteria associated with mosquitoes. Our analysis

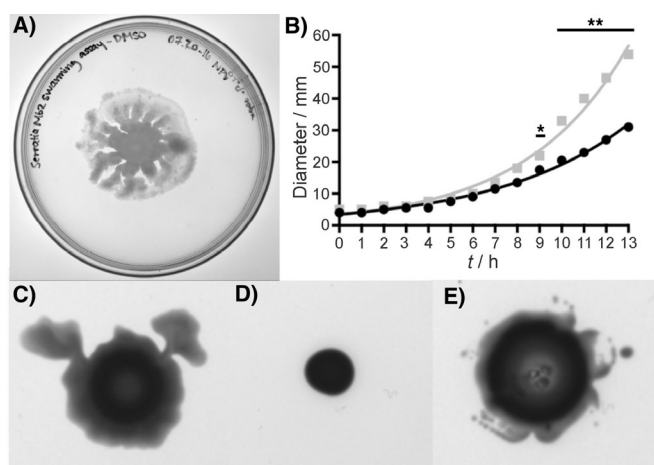


Figure 3. A) WT *Serratia* sp. swarming. B) *Serratia* sp. swarming diameter as a function of time with stephensiolides added (1 μL of 1 mg mL^{-1} solution; \blacksquare) and without (DMSO; \bullet). Experiment completed with two biological replicates (* $p \leq 0.05$, ** $p \leq 0.01$). Error bars represent the standard error of the mean. For the swarming data points, the error bars are shorter than the height of the symbol. C) WT *S. marcescens* CMS376 swarming. D) Non-swarming mutant of *S. marcescens* CMS376. E) Swarming phenotype is rescued in non-swarming mutant when stephensiolides are added exogenously.

revealed that the stephensioides aid in bacterial swarming motility, likely strengthening the bacteria's ability to populate *Anopheles* mosquitoes as well as other hosts where the stephensioides are produced. Together, these findings set the foundation for future examination of the mosquito microbiome to enhance our understanding of the complex inter-species relationship that contributes to transmission of vector-borne infectious agents, like the *Plasmodium* parasite.

Acknowledgements

We are grateful to Duke University for sponsoring this research. We thank Drs. Mohammad Seyedsayamdost, Pierre Stallforth, and Jiyong Hong for useful discussion, Dr. Robert Shanks for supplying *S. marcescens* CMS376 and CMS635, Drs. George Dubay and Peter Silinski for mass spectrometry assistance, Dr. Anthony Ribeiro and the Duke NMR Facility for assistance, Kelsey Morgan and Dr. Dewey McCafferty for preparative HPLC assistance, and Nishma Vias for aid with swarming assays.

Conflict of Interest

The authors declare no conflict of interest.

Keywords: lipodepsipeptides • microbiome • mosquitoes • natural products

- [1] J. J. Scott, D.-C. Oh, M. C. Yuceer, K. D. Klepzig, J. Clardy, C. R. Currie, *Science* **2008**, *322*, 63.
- [2] D.-C. Oh, M. Poulsen, C. R. Currie, J. Clardy, *Nat. Chem. Biol.* **2009**, *5*, 391–393.
- [3] G. Carr, M. Poulsen, J. L. Klassen, Y. Hou, T. P. Wyche, T. S. Bugni, C. R. Currie, J. Clardy, *Org. Lett.* **2012**, *14*, 2822–2825.
- [4] S. Sood, H. Steinmetz, H. Beims, K. I. Mohr, M. Stadler, M. Djukic, W. von der Ohe, M. Steinert, R. Daniel, R. Müller, *ChemBioChem* **2014**, *15*, 1947–1955.
- [5] World Health Organization, *Vector-Borne Diseases*, **2016**, www.who.int/en/news-room/fact-sheets/detail/vector-borne-diseases.
- [6] A. Boissière, M. T. Tchioffo, D. Bachar, L. Abate, A. Marie, S. E. Nsango, H. R. Shahbazkia, P. H. Awono-Ambene, E. A. Levashina, R. Christen, I. Morlais, *PLoS Pathog.* **2012**, *8*, e1002742.
- [7] B. Weiss, S. Aksoy, *Trends Parasitol.* **2011**, *27*, 514–522.
- [8] Y. Dong, F. Manfredini, G. Dimopoulos, T. Tchuinkam, B. Faas, *PLoS Pathog.* **2009**, *5*, e1000423.
- [9] C. M. Cirimotich, Y. Dong, A. M. Clayton, S. L. Sandiford, J. A. Souza-Neto, M. Mulenga, G. Dimopoulos, *Science* **2011**, *332*, 855858.
- [10] A. Iguchi, Y. Nagaya, E. Pradel, T. Ooka, Y. Ogura, K. Katsura, K. Kurokawa, K. Oshima, M. Hattori, J. Parkhill, et al., *Genome Biol. Evol.* **2014**, *6*, 2096–2110.
- [11] A. Rani, A. Sharma, R. Rajagopal, T. Adak, R. K. Bhatnagar, *BMC Microbiol.* **2009**, *9*, 96.
- [12] P. Kukutla, B. G. Lindberg, D. Pei, M. Rayl, W. Yu, M. Steritz, I. Faye, J. Xu, *Genome Announc.* **2013**, *1*, e01030-13.
- [13] P. Sharma, S. Sharma, R. Maurya, T. De, T. Thomas, S. Lata, N. Singh, K. Pandey, N. Valecha, R. Dixit, *Parasit. Vectors* **2014**, *7*, 235.
- [14] J. Masschelein, M. Jenner, G. L. Challis, *Nat. Prod. Rep.* **2017**, *34*, 712–783.
- [15] J. W. de Haan, L. J. M. Van de Ven, *Org. Magn. Reson.* **1973**, *5*, 147–153.
- [16] R. M. Silverstein, F. X. Webster, D. J. Kiemle, *Spectrometric Identification of Organic Compounds*, 7th ed., Wiley, Hoboken, **2005**, pp. 198.
- [17] P. Marfey, *Carlsberg Res. Commun.* **1984**, *49*, 591–596.
- [18] M. A. Fischbach, C. T. Walsh, *Chem. Rev.* **2006**, *106*, 3468–3496.
- [19] M. A. Skinnider, C. A. Dejong, P. N. Rees, C. W. Johnston, H. Li, A. H. Webster, M. A. Wyatt, N. A. Magarvey, *Nucleic Acids Res.* **2015**, *111*, 9645–9662.
- [20] X. Yin, T. M. Zabriskie, *Microbiology* **2006**, *152*, 2969–2983.
- [21] T. Weber, K. Blin, S. Duddela, D. Krug, H. U. Kim, R. Brucoleri, S. Y. Lee, M. A. Fischbach, R. Müller, W. Wohlleben, R. Breitling, E. Takano, M. H. Medema, *Nucleic Acids Res.* **2015**, *43*, W237–W243.
- [22] C. J. Balibar, F. H. Vaillancourt, C. T. Walsh, *Chem. Biol.* **2005**, *12*, 1189–1200.
- [23] S. A. Sieber, M. A. Marahiel, *Chem. Rev.* **2005**, *105*, 715–738.
- [24] R. H. Dadd, *J. Insect Physiol.* **1975**, *21*, 1847–1853.
- [25] E. Crotti, A. Rizzi, B. Chouaia, I. Ricci, G. Favia, A. Alma, L. Sacchi, K. Bourtzis, M. Mandrioli, A. Cherif, C. Bandi, D. Daffonchio, *Appl. Environ. Microbiol.* **2010**, *76*, 6963–6970.
- [26] B. Chouaia, P. Rossi, S. Epis, M. Mosca, I. Ricci, C. Damiani, U. Ulissi, E. Crotti, D. Daffonchio, C. Bandi, G. Favia, *BMC Microbiol.* **2012**, *12*, S2.
- [27] I. Wiegand, K. Hilpert, R. E. W. Hancock, *Nat. Protoc.* **2008**, *3*, 163–175.
- [28] D. M. Citron, M. D. Appleman, *J. Clin. Microbiol.* **2006**, *44*, 3814–3818.
- [29] S. Balakrishnan, K. Indira, M. Srinivasan, *J. Parasit. Dis.* **2015**, *39*, 385–392.
- [30] N. A. Broderick, K. F. Raffa, J. Handelsman, *Proc. Natl. Acad. Sci. USA* **2006**, *103*, 15196–15199.
- [31] C. Berry, *J. Invertebr. Pathol.* **2012**, *109*, 1–10.
- [32] M. Yiallourou, V. Storch, I. Thiery, N. Becker, *J. Am. Mosq. Control Assoc.* **1994**, *10*, 51–55.
- [33] P. W. Lindum, U. Anthoni, C. Christophersen, L. Eberl, S. Molin, M. Givskov, *J. Bacteriol.* **1998**, *180*, 6384–6388.
- [34] H. Li, T. Tanikawa, Y. Sato, Y. Nakagawa, T. Matsuyama, *Microbiol. Immunol.* **2005**, *49*, 303–310.
- [35] T. Matsuyama, T. Murakami, M. Fujita, S. Fujita, I. Yano, *Microbiology* **1986**, *132*, 865–875.
- [36] D. B. Kearns, *Nat. Rev. Microbiol.* **2010**, *8*, 634–644.
- [37] R. M. Q. Shanks, N. A. Stella, R. M. Lahr, S. Wang, T. I. Veverka, R. P. Kowalski, X. Liu, *PLoS One* **2012**, *7*, e36398.
- [38] S. Wang, A. L. A. Dos-Santos, W. Huang, K. C. Liu, M. A. Oshaghi, G. Wei, P. Agre, M. Jacobs-Lorena, *Science* **2017**, *357*, 1399–1402.
- [39] S. F. Altschul, W. Gish, W. Miller, E. W. Myers, D. J. Lipman, *J. Mol. Biol.* **1990**, *215*, 403–410.
- [40] H. S. Sader, D. J. Farrell, R. K. Flamm, R. N. Jones, *Int. J. Antimicrob. Agents* **2014**, *43*, 328–334.

Manuscript received: March 7, 2018

Accepted manuscript online: April 26, 2018

Version of record online: June 10, 2018